Interfacial tensions of industrial fluids from a molecular-based square gradient theory

José Matías Garrido and Andrés Mejía*

Departamento de Ingeniería Química,

Universidad de Concepción, POB 160-C, Concepción, Chile

Manuel M. Piñeiro

Departamento de Física Aplicada, Facultade de Ciencias,

Universidade de Vigo, E36310, Vigo, Spain

Felipe J. Blas

Laboratorio de Simulación Molecular y Química Computacional,

CIQSO-Centro de Investigación en Química

Sostenible and Departamento de Física Aplicada,

Universidad de Huelva, 21007 Huelva, Spain

Erich A. Müller†

Department of Chemical Engineering,

Imperial College London, South Kensington Campus,

London SW7 2AZ, United Kingdom

(Dated: January 28, 2016)

Abstract

This work reports a procedure for predicting the interfacial tension of pure fluids. It is based on scaling arguments applied to the influence parameter of the van der Waals theory of inhomogeneous fluids. The molecular model stems from the application of the Square Gradient Theory to the SAFT-VR Mie equation of state. The theory is validated against computer simulation results for homonuclear pearl-necklace linear chains made up to six Mie $(\lambda-6)$ beads with repulsive exponents spanning from $\lambda = 8$ to 44 by combining the theory with a corresponding states correlation to determine the intermolecular potential parameters. We provide a predictive tool to determine interfacial tensions for a wide range of molecules including hydrocarbons, fluorocarbons, polar molecules, among others. The proposed methodology is tested against comparable existing correlations in the literature, proving to be vastly superior, exhibiting an average absolute deviation of 2.2 %.

* amejia@udec.cl

† e.muller@imperial.ac.uk

INTRODUCTION

Interfacial tension (IFT) is arguably the key thermophysical property that governs the behaviour of inhomogeneous fluids. Its relevance is rooted in the fact that the magnitude of the IFT and its relationship to other state variables (*i.e.*, temperature, pressure, composition) controls several interfacial phenomena such as wetting transitions, interfaces at the vicinity of critical states, nucleation of new phases, etc. The physical understanding and modelling of IFT also provides a route to link tensions with the inhomogeneous behaviour of fluids at molecular level, such as concentration of species along the interfacial zone, interfacial width, etc.[1,2] An additional distinctive characteristic of the IFT is that its value can be obtained from experimental measurements,[3] molecular simulations,[4] and theoretical approaches.[1,3,5,6] Specifically, experimental determinations can be carried out by using tensiometers. In these devices, the IFT is indirectly measured from the force needed to detach an object from a free surfaces (e.g., Wilhelmy plate and du Noüy ring tensiometers) or by combining Laplace's equation with some characteristic dimensions of the system, such as the liquid height in a capillary tube (e.g., capillary rise tensiometer) or the silhouette of a pendant or ellipsoid drop (e.g., pendant drop and spinning drop tensiometers, respectively). For further discussions related to tensiometers and the experimental techniques the reader is redirected to Refs.[3and7]. From a molecular simulation perspective, inhomogeneous fluids can be simulated in the canonical ensemble by using both Molecular Dynamics and Monte Carlo schemes.[4] In both schemes, the IFT can be computed from the mechanical and/or the thermodynamic route. In the mechanical route or IK method[8], the IFT is computed from the integration of the difference between the normal and tangential pressure (Hulshof's integral[9]), which are described by the diagonal components of the Irving and Kirkwood tensor.[10] In the thermodynamic route or Test Area method[11], the IFT is computed from the change in the Helmholtz energy in the limit of an infinitesimal perturbation in the interfacial area. Empirically, IFT can be related to the difference between the liquid and vapor densities through a phenomenological relationship know as the Parachor.[12,13] Such an approach is useful from a practical standpoint, buy its lack of rigour precludes any meaningful extrapolation. From a more fundamental viewpoint, the calculation of the IFT can be based on corresponding states principles[14,15] and statistical mechanics perturbation methods[6], where the Square Gradient Theory (SGT)[16,17] stands out as one of the most widely used. From a formal perspective,

classical density functional theory (DFT) also provides a route to determine density profiles and IFT in simple scenarios, but it us yet to be fully developed for non-spherical fluids.[18–21] In SGT, the Helmholtz energy density of the interfacial fluid is described by the sum of two contributions. The first part takes into account the Helmholtz energy density for the homogeneous fluid at a local-density, while the second part represents the inhomogeneous contribution of Helmholtz energy by a product of square local-density gradients and some characteristic parameters. These latter parameters have been historically called influence parameters since their values govern the stability and characteristic length scales of the interfaces. The popularity of SGT can be attributed to its relative simplicity and to the unique proposition of using the same equation of state to model simultaneously the homogeneous (*e.g.*, phase equilibria) and inhomogeneous (interfacial properties) behaviour of fluids in a good agreement with experimental data. Additionally, SGT provides other interfacial properties such as density or concentration profiles along the interfacial zone, interface thickness, excess adsorption, surface enthalpy and surface entropy, etc. The physical reliability of SGT has been verified by several authors for pure fluids and multicomponent fluid mixtures in different phase equilibria scenarios, such as vapour-liquid, liquid-liquid, vapour-liquid-liquid and four phases. All these calculations have been carried out by using a myriad of equations of state (EoS) to model the homogeneous part of the interfacial Helmholtz energy. A representative but not exhaustive list of the most common used EoS are cubic van der Waals -type EoS.[22–37], cubic plus association (CPA) EoS[38–40], non-cubic EoS[41], technical EoS[42] and molecular based EoS[43–71].

Despite the success of SGT for describing interfacial properties of pure fluids and fluid mixtures, this theory depends crucially on the independent determination of the influence parameter. Theoretically, the influence parameter can be computed from its molecular definition (*i.e.*, integration of the direct correlation function of the homogeneous fluid), but the available theories for the two-body direct correlation function between two species in homogeneous fluids are not completely developed, as the results still exhibit poor performance when compared to experimental or molecular dynamics results.[72–75] To circumvent this problem, Carey[22,76] proposed to invest the problem and back-calculate the influence parameter using experimental data of IFT and SGT to later correlate the results to the EoS parameters. This semi empirical approach has been broadly used for pure fluids and nowadays quite refined correlations are available. For instance, Zuo and Stenby[27], Miqueu

et al.[29] and Lin *et al.*[34], have used the Peng - Robinson EoS[77] and its volume translated version in SGT to correlate the influence parameter as a function of temperature and the acentric factor. These correlations have shown a remarkably good agreement between SGT estimations and experimental data. The same procedure has been also used starting from molecular based EoS, such as SAFT EoS and its variants, where both experimental data and Molecular Dynamics simulations have been used to correlated the influence parameter (see for instance Refs.[48,53,71,and78]). Mixtures add another dimension of complexity, whereas the corresponding binary (cross) influence parameter must then be determined, usually in an empirical fashion through simple geometric mixing rules or by fitting to binary experimental data. This approach seems to work for most simple cases and is trivially extendable to multicomponent mixtures.

In summary, while SGT is a powerful theory for describing the interfacial tension of pure fluids and fluid mixtures its main limitation for it to be used as a predictive theory is the lack of generality and limited transferability of the influence parameters. The main goal of this work is to develop a flexible, transferable and universal set of relations for the influence parameter for pure fluids. A rather long-standing affort has been made to produce a molecular-based equation of state that can faithfully represent in a quantitative fashion the macroscopic thermodynamic properties of fluids with these potentials. The latest version of these theories, the SAFT-Mie equations[79,80], which will be discussed later, has been sucessfully employed both as a tool for fitting, correlating and subsequent prediction of fluid phase equilibria in a wide range of scenarios (e.g. vapor-liquid equilibria, water-octanol partition coefficients, liquid-liquid equilibria, etc.) for a wide range of industrially relevant fluids including, but not limited to polar fluids, refrigerants, crude oils, polymers, etc. However, possibly, the most interesting feature of these equations is the direct and quantitative link to the underlying potential, such that information gathered experiments can be incorporated into intermolecular potentials of interest here, is to garner experience from the molecular simulation of vapor-liquid interfaces to directly feed into this framework, in order to build a robust and transferable model capable of predicting the properties of an interfacial system from a minimal amount of commonly available experimental information, such as critical constants (see Refs.[65–67,81–87] for a complete discussion).

This paper is organized as follows: We summarize the main working expressions of the SGT and the SAFT-VR Mie EoS in Section II. In Section III we briefly consider the Molecular

simulation methodology used in this work. The main results obtained from the corresponding states correlations for interfacial tension and applications for selected fluids are discussed in Section IV. Finally, the main conclusions are summarized in Section V.

THEORY

The Square Gradient Theory for fluid interfaces

The Square Gradient Theory (SGT) for fluid interfaces was proposed by van der Waals in the early 1890s, with the original paper published in 1894[16] after he confirmed the reliability of this theory by describing the observed experimental data of pure ether near to the critical state measured by de Vries in 1893.[88] In the original work, van der Waals proposed for the first time a smooth density variation through the interface region rather than a infinitely sharp variation proposed by Laplace. For a complete historical description of the origin and motivations involved in the development of SGT and also its similarities to the work of Rayleigh and Fuchs on capillarity, the reader is redirected to the books by Kipnis *et al.*[89] Levelt Sengers[90] and Rowlinson[91] and Rowlinson and Widom[1]. The SGT was rediscovered and extended for mixtures by Cahn and Hilliard sixty years later.[92] In the middle of 70s, the SGT was remasterized simultaneously and independently by Bongiorno and Davis[73,74] and Yang *et al.*[93] by using statistical mechanics arguments. However, its popularity rises at the end of 70s, when Carey[22,23,76] gave a boost to SGT by applying it to the Peng-Robinson EoS[77] and reported interfacial properties for both pure fluids and fluid mixtures. Since Carey's seminal work, multiple authors have used SGT to describe interfacial properties for pure fluids and multicomponent mixtures in biphasic, triphasic and multi-phasic phase equilibrium. In fact, according to our records there are more than 150 scientific papers related to SGT and this theory has been used as base for several PhD thesis (see for example Refs.[76,94–98]). As SGT has been broadly discussed in the literature, this section only condenses the main working expressions for modeling the interfacial behavior for the case of pure fluids in vapor - liquid equilibrium. The reader is directed Refs.[99and100] and the corresponding PhD thesis for a complete deduction of SGT.

In the SGT, the interfacial density of a pure fluid, $\rho(z)$, varies continuously from the bulk density of a vapor ($\rho(z \to -\infty) = \rho^V$) to the bulk density of a liquid ($\rho(z \to +\infty) = \rho^L$). In

order to describe this continuous evolution, van der Waals proposed to express the Helmholtz energy (A) of an interfacial or inhomogeneous fluid as a second order Taylor expansion about the homogenous Helmholtz energy density, a_0, at the local density ρ. For the case of pure fluids characterized by flat interfaces between adjacent phases, the Taylor expansion may be performed along the interface width by considering a normal z-coordinate (perpendicular to the plane of the interface) as follows:

$$A = S \int_{-\infty}^{+\infty} \left[a_0 \left(\rho \left(z \right) \right) + \frac{1}{2} c \left(\frac{d\rho \left(z \right)}{dz} \right)^2 \right] dz \tag{1}$$

where S corresponds to the interfacial area and c denotes the influence parameter. In this expression, the first term within the integral refers to the homogeneous fluid contribution and the second term corresponds to the inhomogeneous part expressed as gradient term multiplied by the influence parameter (c). The minimization of Equation (1) for a closed system leads to the following second order differential equation of $\rho \left(z \right)$:

$$\frac{d}{dz} \left[\frac{c}{2} \left(\frac{d\rho}{dz} \right)^2 \right] = \frac{d\Omega \left(\rho \right)}{dz} \tag{2}$$

in Equation (2), Ω represents the grand thermodynamic potential, which is defined as $\Omega \left(\rho \right) = a_0 \left(\rho \right) - \rho \left(\partial a_0 / \partial \rho \right)^0$, where the superscript denotes that the term is evaluated at phase equilibrium conditions, and a_0 is the molar Helmholtz energy.

Considering the boundary conditions for a planar interface in vapour-liquid equilibrium (*i.e.*, $\rho \left(z \to +\infty \right) = \rho^L$, $\rho \left(z \to -\infty \right) = \rho^V$ and $d\rho / dz \left(z \to \pm\infty \right) = 0$), the integration of Equation (2) yields to the interfacial density profile:

$$z - z_0 = \int_{\rho_0}^{\rho(z)} \sqrt{\frac{c}{2 \left(\Omega - \Omega^0 \right)}} d\rho \tag{3}$$

where z_0 is an arbitrary spatial coordinate for the bulk density ρ_0. Ω^0 denotes the grand thermodynamic potential at equilibrium where $\Omega^0 = \Omega^0 \left(\rho^L \right) = \Omega^0 \left(\rho^V \right) = -P^0$ and P^0 is the bulk equilibrium pressure (or vapor pressure).

Within the SGT (cf. Equation (1)), the interfacial tension, γ, between vapor - liquid phases can be computed from the following expression:

$$\gamma = \left(\frac{\partial A}{\partial S} \right)_{TVN} = \int_{-\infty}^{+\infty} c \left(\frac{d\rho}{dz} \right)^2 dz \tag{4}$$

Alternatively, the interfacial tension of pure fluids can be also calculated by using the following integral expression, which is obtained by combining Equation (3) and Equation (4):

$$\gamma = \int_{\rho^V}^{\rho^L} \sqrt{2c\left(\Omega + P^0\right)} d\rho \tag{5}$$

Inspection of Equations (3) to (5) reveals that the calculation of $\rho\left(z\right)$ and γ depend on the EoS model and crucially, on the undetermined parameter c.

The Statistical Associating Fluid Theory (SAFT) EoS

As is obvious from above, one of the key inputs of SGT is the EoS model. The EoS model not only provides a model for a_0 but also a framework to calculate the phase equilibrium and the corresponding bulk phase densities. Following Carey's seminal work describing the procedure to link modern EoS to SGT, several EoSs have subsequently been used in SGT, being the Peng - Robinson EoS[77] and SAFT EoS the most popular choices. In this context, the main advantage of cubic EoSs is their mathematic simplicity and the parametrization of their parameters in terms of critical coordinates and acentric factor. However, cubic EoSs display well documented limitations for simultaneous fitting both liquid densities, vapor pressures and critical points. This limitation can be circumvented by using more sophisticated molecular EoS models such as the SAFT EoS (see McCabe and Galindo[101] for a recent review on this EoS).

In this work, we select the most update version of SAFT, the SAFT-VR-Mie EoS,[79] which represents a significative advance in SAFT models.[102] The main improvement of this version versus older encarnations is the expression up to third order in the residual Helmholtz energy of the monomer term and the flexibility brought about by being based on the Mie potential[103], u^{Mie}, which can be represented by

$$u^{Mie}\left(r_{ij}\right) = C\varepsilon\left[\left(\frac{\sigma}{r_{ij}}\right)^{\lambda_r} - \left(\frac{\sigma}{r_{ij}}\right)^{\lambda_a}\right] \tag{6}$$

In Equation (6), λ_r and λ_a are the repulsion and attraction parameters of the intermolecular potential, respectively, r_{ij} is the center-to-center distance of the interacting segments, ε is the energy scale corresponding to the potential well depth, σ is the length scale, corresponding loosely with an effective segment diameter, and C is a constant defined as:

$$C = \frac{\lambda_r}{\lambda_r - \lambda_a} \left(\frac{\lambda_r}{\lambda_a}\right)^{\frac{\lambda_a}{\lambda_r - \lambda_a}} \tag{7}$$

The Mie potential reverts to the well-known Lennard-Jones model[104] if the repulsive and attractive exponents are taken as 12 and 6, respectively. The expression of the Helmholtz energy density of SAFT-VR Mie EoS for a non associating chain fluid is given by[79]

$$a_0 = \left(a^{IDEAL} + a^{MONO} + a^{CHAIN}\right) \rho \frac{N_{av}}{\beta} \tag{8}$$

where $a = A/(Nk_BT)$ and A is the total Helmholtz energy, N is the total number of molecules, N_{av} is the Avogadro constant, T is the temperature, k_B is the Boltzmann constant, $\beta = 1/(k_BT)$, and ρ is the molar density of the fluid. a^{MONO} represents monomer (unbounded) contribution for a chain composed of m_s tangential segments, a^{CHAIN} accounts for the formation of chain molecules and a^{IDEAL} is the ideal gas contribution. For a complete overview of this model the reader is referred to Ref.[79].

Coarse-graining of fluid potential using SAFT

In this work, the pure fluids are modelled as freely jointed tangential non associating spheres (pearl-necklace model) characterized by five parameters: m_s, λ_r, λ_a, ε, and σ, which can be found from several routes. One could be tempted to fit these parameters to the properties of a lower resolution model, e.g. a fully atomistic classic molecular model of the Optimized Potentials for Liquid Simulations (OPLS) family[105] . As the models proposed here are of lower fidelity some degrees of freedom would have to be factored out during this procedure which would result in a coarse grained (CG) model that is usually state dependent and unreliable. An alternative approach is to use the equation of state to fit macroscopic experimental thermophysical properties that derive from the Helmholtz energy, such as pressures and densities along the vapour-liquid saturation curve. This approach provides a pathway for obtaining robust parameters that describe the average pairwise interactions. An implicit assumption is that the equation of state describes precisely the underlying Hamiltonian, which is the case in the version of SAFT employed herein. This top-down CG parametrization is discussed in detail by Müller and Jackson[84]. Talking this approach further, Mejía *et al.*[106] expressed the SAFT-VR Mie EoS in a corresponding state form

finding explicit links between a small number of well defined properties (critical temperature, acentric factor, and liquid density) and the force field parameters. This latter procedure is followed herein. The number of beads, m_s, that describe a molecular model is determined beforehand by observation of the molecule geometry. The underlying model requires the bead to be tangent to each other and in a linear configuration (pearl-necklace model). Ramrattan *et al.*[107] have shown that there is a conformality relationship between the exponents of the Mie potential; an infinite number of exponent pair (λ_a, λ_r) will provide essentially the same field phase behaviour. Following this, we chose to fix the attractive potential $\lambda_a = 6$[108] leaving the repulsive exponent $\lambda_r = \lambda$ as the lone parameter that defines the range of the intermolecular potential.

Once the EoS parameters have been fixed, Equation (8) is used to predict the vapor - liquid phase equilibrium according to the conditions of isothermal phase equilibrium for bulk phases:[36]

$$\Omega\left(\rho^V\right) = \Omega\left(\rho^L\right) = -P^0 \tag{9}$$

$$\left(\frac{\partial \Omega}{\partial \rho}\right)_{T^0,V^0} = \left(\frac{\partial a_0}{\partial \rho}\right)_{T^0,V^0} - \left(\frac{\partial a_0}{\partial \rho}\right)^0 \tag{10}$$

$$\left(\frac{\partial^2 \Omega}{\partial \rho^2}\right)_{T^0,V^0} = \left(\frac{\partial^2 a_0}{\partial \rho^2}\right)_{T^0,V^0} > 0 \tag{11}$$

Equation (9) corresponds to the mechanical equilibrium condition ($P^0 = P^L = P^V$), Equation (10) expresses the chemical potential constraint ($(\partial a_0/\partial \rho)_{T,V} \equiv \mu$, $\mu^0 = \mu^L = \mu^V$), and Equation (11) is a differential stability condition for interfaces, comparable to the Gibbs energy stability constraint of a single phase.[36]

The influence parameter

In the original van der Waals theory, the influence parameter, c, is defined as a constant, but modern versions of this theory reflect that this parameter should be a function of the direct correlation function of the homogeneous fluid. According to Bongiorno *et al.*,[73] and Yang *et al.*,[93] the rigorous definition of c is given by the following integral expression:

$$c = \frac{k_B N_{av}^2 T}{6} \int_V r^2 c^0 (r;\rho)\, dV \tag{12}$$

where $c^0(r;\rho)$ is the direct correlation function of homogeneous fluid and r is a spatial coordinate. Since $c^0(r;\rho)$ is intractable from an analytic viewpoint, some models have been developed to estimate the influence parameters from other measurable or computable quantities. According to Rowlinson and Widom,[1] one of the most successful approximations for c^0 is to consider $c^0(r;\rho) \approx c^0(r;T)$ where $c^0(r;T)$ can be described by the Percus - Yevick approximation:[109]

$$c^0 (r;T) = g(r)\left[1 - exp\left(-u(r)/k_B T\right)\right] \tag{13}$$

where $g(r)$ is the radial distribution function of a fluid in the homogeneous state and $u(r)$ is the intermolecular potential, respectively. In a mean field approximation, a locally uniform fluid distribution can be assumed, hence, $g(r) \approx 1$. Linearizing Equation (13), a mean-spherical approximation for the direct correlation function of homogeneous fluid can be obtained:

$$c^0 (r,T) \approx -u(r)/k_B T \tag{14}$$

which if replaced in Equation (12), and considering an isotropic fluid becomes

$$c = -\frac{4\pi N_{av}^2}{6} \int_\sigma^\infty r^4 u(r)\, dr \tag{15}$$

Equation (15) represents the simplest approximate model for c and it acquires a final form once the intermolecular potential is defined. For the case of the Mie potential (cf. Equation (6) and Equation (15)) simplifies to:

$$c = \frac{-2\pi N_{av}^2 C\varepsilon\sigma^5}{3}\left[\left(\frac{1}{\lambda_r - 5}\right) - \left(\frac{1}{\lambda_a - 5}\right)\right] \tag{16}$$

From Equation (16) it follows that c can be treated as a constant once the intermolecular potential exponents (λ_r, λ_a) and fluid parameters (ε, σ) have been defined. Some particular cases of Equation (16) have been used to predict the interfacial behavior of pure fluids and fluid mixtures. For example, $\lambda_r = 12$ and $\lambda_a = 6$ (*i.e.*, the Lennard-Jones potential[104]) has been used by Carey,[22,76] to predict the c value and relate it to the Peng - Robinson

EoS[77] constant (*i.e.*, a and b), whereas Tardón *et al.*,[110]used it to predict the interfacial behavior in asymmetric Lennard-Jones mixtures that display molar isopycnicity inversion. The reported results of concentration profiles show a qualitative agreement between theory and molecular simulations. Other examples include the use of $\lambda_r = -\infty$ and $\lambda_a = 6$ (*i.e.*, the Sutherland potential[111]). This potential has been used by Poser[43,44,95] to describe the interfacial properties of low molecular weight fluids and some polymers and Mejía and Segura[31,32] used it to explore qualitatively the multiphase interfacial behavior of Type IV and Shield region. While a constant c value (cf. Equation (16)) can be used for describing qualitatively the interfacial properties for pure fluids and fluid mixtures, some previous works[48,53,72] based on molecular simulations and SGT have demonstrated that the c values necessary are a function of the shape factor (elongation, chain length, etc.) for non-spherical molecular fluids and seen to vary with temperature. Specifically, Duque *et al.*,[48] have shown that as the molecular chain length increases the c values increases whereas Baidakov *et al.*,[72] and Galliero *et al.*[53] reported values of c as a function of temperature for the case of spherical fluids. In addition, the values calculated from Equation (16) for the case of monomer Lennard-Jones pure fluids display some over-predictions when they are compared to the values obtained from molecular simulation results. As an illustrative example, Equation (16) predicts $c \simeq 7.181\, N_{av}^2 \varepsilon \sigma^5$ for a Lennard-Jones pure fluid which is 1.6 times the value reported by Duque *et al.*,[48].

In summary, the mean-spherical approximation for the direct correlation function of homogeneous fluid provides a route to obtain an analytical expression for c. This expression can be used for qualitative description of interfacial properties from SGT, but requires refinement if it is to be used as a predictive tool. In this work, the refinement of the theory is carried out by exploiting the direct link between EoS and the underlying intermolecular potential. Specifically, molecular simulations of the chain fluids composed of Mie beads are compared to the theory seeking a quantitative agreement. These resulting equations are the base for a molecular thermodynamic framework to correlate the IFT of industrial - relevant fluids.

COMPUTATIONAL METHODS

In order to have a high fidelity data set for molecular fluids, we have carried out Molecular Dynamics (MD) simulations of pure fluid interfacial properties, using the direct coexistence technique in inhomogeneous simulation boxes. We employ here canonical simulations where N molecules at a fixed temperature T are placed in a parallelepipedic simulation cell of constant volume V.[4,112] Following the methodology proposed by Martínez-Veracoechea and Müller[113] all simulations are started from a high temperature homogeneous monophasic system that is quenched abruptly to the simulation temperature until equilibration is reached through diffusive mass transport. In this work, chain molecules are treated as freely-jointed tangent Mie spheres, *i.e.*, bond distances are kept constant at a value of σ and no further intra-molecular interactions are considered. All the sites have the same mass, and interact with each other through an effective pairwise Mie $\lambda_r - 6$ intermolecular potential (c.f. Equation (6)).

MD simulations are performed on systems containing from 6500 to 12600 Mie beads at conditions where the vapor-liquid interface is present. The simulation cell is a $L_x \times L_y \times L_z$ parallelepiped with periodic boundary conditions in all three directions. Specifically, L_x and L_y are parallel to the interfacial surface, while L_z direction is normal to the interface. These values are chosen to ensure a cell large enough to accommodate liquid and gas regions with enough molecules to ensure a representative bulk phase. To guarantee this, L_z was fixed to be much larger than L_x and L_y. Typically $L_x = L_y = 20\sigma$ and L_z is set to be 5 to 7 times larger. In all cases, the two interfaces spontaneously appear in the $x - y$ plane. In order to reduce the potential truncation and system size effects involved in the phase equilibrium and interfacial properties calculations, the cut-off radius (r_c) has been taken equal to a relatively large value of 10σ. It has been shown[53,114,115] that a cut-off above six segment diameters provides a reliable description for the pressure and interfacial properties of the Lennard-Jones fluid and we expect that to translate to Mie fluids.

A modified version of the DLPOLY simulation package (which includes a specific routine to perform pressure components profile calculations) has been used, considering a Verlet-leapfrog[116] algorithm with a time step of 0.003 in reduced units of $\sigma\sqrt{M/\varepsilon}$, where M denotes the particle or atom mass, and a Nose-Hoover thermostat[117,118] with a time constant equal to 1.0 in reduced units of $\sigma\sqrt{M/\varepsilon}$. After the initial temperature quenching, the systems

are equilibrated for 1×10^5 time steps. After this equilibration stage, a production run is performed for at least another 4×10^5 time steps.

In order to characterize the bulk phase and interfacial behavior, density profiles are calculated by dividing the system in 400 slabs along the z direction. The molecular density profiles, $\rho_i(z)$, are obtained by assigning the position of each bead, z_i, to the corresponding slab, and constructing the molecular density from mass balance considerations. Additionally, these profiles are displaced so that the center of mass of the liquid slab lies at the center of the simulation cell, this displacement helps to avoid smearing of the profiles due to fluctuations of the center of mass location. In order to estimate errors on the variables computed, the sub-blocks average method has been applied.[119] In that approach, the production period is divided into n independent blocks. The statistical error is then deduced from the standard deviation of the average divided by $n^{1/2}$. The equilibrium pressure and interfacial tension are obtained using the Irving-Kirkwood method, where the profiles of the pressure tensor diagonal elements are calculated employing the virial expression:[10]

$$P_{kk} = k_B T \rho(z) + \frac{1}{S} \left\langle \sum_{i}^{N-1} \sum_{j>i}^{N} \frac{1}{|z_i - z_j|} (f_{ij})_k (r_{ij})_k \right\rangle \tag{17}$$

where P_{kk} is the pressure tensor elements, the subscript kk represents the spacial coordinate, either x, y, or z, k_B is Boltzmann's constant, T is the absolute temperature, S is the interfacial area, N is the number of molecules, f_{ij} is the force on molecule i due to molecule j, and r_{ij} represents the distance between molecules i and j. f_{ij}, r_{ij} contributions have been equally distributed among the slabs corresponding to each molecule and all the slabs between them. The term $k_B T \rho(z)$ in Equation (17) takes into account the kinetic contribution, which is proportional to the ideal gas pressure. The term into the $\langle \cdots \rangle$ brackets corresponds to the configurational part which is evaluated as ensemble averages and not at instantaneous values. From the pressure elements of Equation (17), the vapor pressure can be determined, corresponding to the P_{zz} element, while the interfacial tension, γ, can be calculated as[9]

$$\gamma_{MD} = \frac{1}{2} \int_{-\infty}^{+\infty} \left[P_{zz}(z) - \frac{P_{xx}(z) + P_{yy}(z)}{2} \right] dz \tag{18}$$

In this expression, the additional factor 1/2 comes from having two interfaces in the system. The specific details related to the technical implementation of the previous expressions and their evaluations have been discussed extensively in the literature (see Refs[8,49,and120] for

further details). This method, based on the mechanical definition of the pressure tensor, has been selected in this case among the diverse alternatives available, as for instance the so-called Test-Area method[11], that produces equivalent results for this type of systems, as demonstrated by Galliero *et al.*[53]

RESULTS AND DISCUSSION

New expression for the influence parameter

The direct correspondence of SAFT-VR-Mie Eos with the results obtained from an exact solution, obtained via molecular simulations, of the macroscopic behavior of the underlying intermolecular potential suggests the possibility of obtaining the influence parameter directly by forcing the SGT+ EoS model to reproduce exactly interfacial tension data, as proposed originally by Carey.[22,76] However, instead of employing data of real fluids. In order to consistently match the SGT to the IFT data, we use the same fluid model in MD and SGT. The advantage of this combination is that the fluid is described by the same five parameters: m_s, λ_r, λ_a, ε, and σ in both approaches. As explained previously, the attractive exponent can be fixed ($\lambda_a = 6$) leaving the repulsive exponent $\lambda_r = \lambda$ as the lone parameter that defines the range of the intermolecular potential, without any loss of generality.[106,107]

In order to combine the MD results of IFT (Equation (18)) to SGT (Equation (5)), we postulate that c is a constant for each particular fluid (*i.e.*, $c = \Im\left(m_s, \varepsilon, \sigma, \lambda, 6\right)$). If so, the influence parameter can be regressed from the integral (Equation (5)). It proves valuable to express the IFT from MD (Equation (18)) and SGT (Equation (5)) in reduced variables:

$$\gamma^*_{MD} = \frac{1}{2}\int_{-\infty}^{+\infty}\left[P^*_{zz}\left(z^*\right) - \frac{P^*_{xx}\left(z^*\right) + P^*_{yy}\left(z^*\right)}{2}\right]dz^* \tag{19}$$

$$\gamma^*_{SGT} = \frac{1}{m_s}\sqrt{\frac{2c}{\varepsilon\sigma^5}}\int_{\rho^{*,V}}^{\rho^{*,L}}\sqrt{\left(\Omega^* + P^{*,0}\right)}d\rho^* \tag{20}$$

Of course, both equations, Equation (19) and Equation (20), must provide the same numerical results as we compare the exact results from MD to those predicted from the theory. The integral on the right hand side of Equation (20) can be evaluated without recourse to specifying a particular value of the influence parameter, hence a plot of the tension calculated through MD (γ^*_{MD}) as a function of the $\int_{\rho^{*,V}}^{\rho^{*,L}}\sqrt{2\left(\Omega^* + P^{*,0}\right)}d\rho^*$ provides a means of

evaluating the prefactor of Equation (20), namely $\frac{1}{m_s}\sqrt{\frac{c}{\varepsilon\sigma^5}}$. Since m_s, ε and σ are specified a priori, the procedure provides an explicit value of the influence parameter.

Figure 1 shows the results from MD vs. SGT (*i.e.* γ^*_{MD} vs. $\int_{\rho^{*,V}}^{\rho^{*,L}} \sqrt{2\left(\Omega^* + P^{*,0}\right)} d\rho^*$) for pure fluids with different molecular chain length (*i.e.*, $m_s = 1$ to $m_s = 6$) and some selected values of λ (Figure 1(a): $\lambda = 8$; Figure 1(b): $\lambda = 10$; Figure 1(c):, $\lambda = 12$; Figure 1(d): $\lambda = 20$). Simulation and theory results span a wide range of temperatures and chain lengths. Figure 1 evidences a remarkable linear dependence between the ordinate and the abscissa for each Mie $\lambda-6$ fluid, up to a chain length value $m_s = 6$. The slope of these curves corresponds to the term: $(1/m_s)\sqrt{c/\varepsilon\sigma^5}$. In other words, the straight lines in Figure 1 can be used to regress a temperature-independent influence parameter. This behavior clearly evidences a quasi-perfect universal behavior, which had already been predicted using scaling laws and was suggested from a corresponding states viewpoint. Particularly, Blas and co-workers have presented results[121–124] studying the interfacial properties for the Lennard-Jones fluids (for both flexible and rigid chains) showing a similar agreement. Galliero[114] also reported similar behavior by using a corresponding states approach for the case of short flexible Lennard-Jones chains, composed of up to 5 segments.

In the Supporting Information we summarizes the numerical values of the slopes for Mie $\lambda - 6$ fluids as a function of λ. (see table S. I). The challenge is to be able to generalise these results. Recently, Ramrattan *et al.*,[107] pointed out that the behaviour of Mie fluids is governed by the value of the integrated cohesion energy captured by the so-called the van der Waals constant, α, defined as:[125]

$$\alpha = \frac{1}{\varepsilon\sigma^3}\int_{\sigma}^{\infty} u\left(r\right) r^2 dr = C\left[\left(\frac{1}{\lambda_a - 3}\right) - \left(\frac{1}{\lambda_r - 3}\right)\right] \tag{21}$$

Considering a constant value for the attractive exponent ($\lambda_a = 6$), the value of the repulsion exponent is $\lambda_r = \lambda$ and the latter expression reduces to:

$$\alpha = \frac{\lambda}{3\left(\lambda - 3\right)}\left(\frac{\lambda}{6}\right)^{6/\lambda - 6} \tag{22}$$

From the results presented in table S. I presented in supplementary information, it is possible to observe that $(1/m_s)\sqrt{c/\varepsilon\sigma^5}$ decreases with α, for a extended range of repulsive exponents. Indeed, from this analysis the term $(1/m_s)\sqrt{c/\varepsilon\sigma^5}$ can be correlated linearly with the van der Waals constant, α, and thus, we propose the following generalized function

for the influence parameter of Mie $\lambda - 6$ chains fluids:

$$\sqrt{\frac{c}{N_{av}^2 \varepsilon \sigma^5}} = m_s \left(0.12008 + 2.21979\alpha\right) \tag{23}$$

Equation (23) is a general expression for the calculation of the influence parameter, valid for $m_s = 1$ to 6 and $\lambda = 8$ to 38.

It is interesting to point out the differences between the estimation of influence parameters presented here to the results published using previous versions of SAFT-VR Mie[126,127] coupled with SGT. In this work, we obtain a temperature-independent influence parameter for very soft potentials such as for instance the Mie (8-6) fluid, even when chain length increases (c.f. Figure 1(a)). For the same soft potential, Galliero *et al.*,[53] have obtained a different behaviour using a previous SAFT-VR Mie model. In fact, they reported a strongly temperature dependent influence parameter, especially when the fluid is approaching the critical region. Presumably this thermal dependence of the influence parameter is an artifact product of the inability of previous SAFT models to represent accurately the critical and near-critical region[128]. The success of the current version of the SAFT theory relies on the extraordinary ability of the third-order expansion term proposed by Lafitte *et al.*[79] to produce a satisfactory description of VLE near the critical region.

Interfacial Properties for Molecular Fluids

The correlation proposed above is validated by comparing the results obtained from the SGT + SAFT-VR Mie EoS to MD simulation results for the same molecular models (*i.e.*, Mie chains of variable repulsive exponent value and number of segments). Specifically, we test the accuracy of Equation (23) for use within the theory for predicting interfacial properties, such as interfacial density, $\rho_s^* = \rho_s \sigma^3$, profile along the interfacial region, $z^* = z/\sigma$ and interfacial tension, $\gamma^* = \gamma \sigma^2 / \varepsilon$. Figure 2 shows the $\rho_s^* - z^*$profiles for the case of molecular chain fluids ($m_s = 2, 3, 4,$ and 5) interacting by a Mie (10-6) potential. As expected, as the temperature increases, the interfacial region becomes wider, however the take-home message from these figures is the very good agreement between MD and SGT with the influence parameter calculated from Equation (23). In addition to the interfacial profiles in Figure 3 we display the interfacial tension as a function of temperature ($\gamma^* - T^*$) for molecular chain fluids ($m_s = 1$ to 6) interacting through a Mie $(\lambda, 6)$ potential with $\lambda = 8, 10, 12, 20$. From

Figure 3 it is possible to observe that at fixed Mie $(\lambda, 6)$ and m_s, the interfacial tension decreases as the temperature increases, showing a characteristic hyperbolic tangent curve near to the critical state. From these figures, it evident how for a fixed value of the Mie $(\lambda, 6)$ potential, the interfacial tension increases with m_s. Again the key issue evident in Figure 3 is the excellent quantitative agreement between both approaches (MD and SGT), over a wide range of repulsive exponents, molecular chain lengths and temperature, including a satisfactory description near the critical region. The average absolute deviation of the results displayed in Figure 3 are 2.8 % for Mie (8, 6), 1.67% for Mie (10, 6), 1.28 % for Mie (12, 6) and 2.31% for Mie (20, 6).

As a comparison, Figure 3(c) includes the $\gamma^* - T^*$ results for the case of Lennard-Jones chain fluid Mie (12-6) reported by Duque *et al.*[48]. The results reported here display a better agreement to MD results than those reported by Duque *et al.*,[48] particularly for the longer chains.

Corresponding States correlations for interfacial tension

An essential part of the seminal work of van der Waals is the idea that the properties of fluids could be scaled with respect to those of the critical point, providing a meas of reporting a universal behaviour reffered to as the corresponding states principle. For the case of interfacial tension, γ, van der Waals[16] used the critical pressure (P_c) and critical temperature (T_c) of the fluid to form the dimensionless group $\gamma/P_c^{2/3}T_c^{1/3}$ and he proposed to correlate it with $(1 - T/T_c)$. Based on the van der Waals ideas, some authors have used the corresponding state principia to propose interfacial tension correlations. According to Poling *et al.*,[13] the most popular correlations, based on the corresponding state principia, are the Brock and Bird[129], Pitzer,[130] Zuo and Stenby,[131] and Sastri and Rao.[132]

Specifically, Brock and Bird[129] have correlated γ as a function of P_c, T_c and the normal boiling temperature (T_b) for nonpolar fluids:

$$\frac{\gamma}{P_c^{2/3}T_c^{1/3}} = (0.132\,\alpha_c - 0.279)\,(1 - T_r)^{11/9} \tag{24}$$

In Equation (24) T_r is the reduced temperature $(T_r = T/T_c)$ and α_c is the Riedel[133] parameter at the critical point. This parameter has been correlated to P_c and T_b by Miller:[134]

$$\alpha_c = 0.9076 \left[1 + \frac{T_{br}\, ln\left(P_c/1.01325\right)}{1 - T_{br}}\right] \tag{25}$$

In the last expression, T_{br} denotes the reduced normal boiling temperature ($T_{br} = T_b/T_c$). In Equations (24) and (25), the temperature is in Kelvin and the pressure is in bars.

A second popular correlation has been proposed by Curl and Pitzer:[130]

$$\frac{\gamma}{P_c^{2/3} T_c^{1/3}} = \frac{1.86 + 1.18\omega}{19.05} \left[\frac{3.75 + 0.91\omega}{0.291 + 0.08\omega}\right]^{2/3} (1 - T_r)^{11/9} \tag{26}$$

As an extension of the scaling proposed initially by Guggenheim[14], in the Pitzer expression, ω is the acentric factor, which is related to the deviation between the vapor pressure of a given fluid and that of a noble gas. A further correlation for γ has been proposed by Zuo and Stenby.[131] In this work, the authors interpolate between two well-defined reference fluids. The final expression for γ is given by the following expressions:

$$\gamma_r = ln\left(1 + \frac{\gamma}{P_c^{2/3} T_c^{1/3}}\right) \tag{27}$$

$$\gamma_r = \gamma_r^{(a)} + \frac{\omega - \omega^{(a)}}{\omega^{(b)} - \omega^{(a)}} \left(\gamma_r^{(b)} - \gamma_r^{(a)}\right) \tag{28}$$

the superscripts (a) and (b) denote the reference fluids. Zuo and Stenby recommend to use methane $\left(\gamma^{(a)} = 40.520\,(1 - T_r)^{1.287}\right)$ and n-octane $\left(\gamma^{(b)} = 52.095\,(1 - T_r)^{1.21548}\right)$.

According to Poling *et al.*,[13] the methods described previously are satisfactory for nonpolar liquids. For other chemical families, such as alcohol and acids, Poling *et al.*,[13] recommend the use of Sastri and Rao correlation:[132]

$$\gamma = K P_c^x T_b^y T_c^z \left[\frac{1 - T_r}{1 - T_{br}}\right]^m \tag{29}$$

In Equation (29) K, x, y, z, m are constants unique for each chemical family. For example for alcohols: $K = 2.28$, $x = 0.25$, $y = 0.175$, $z = 0$, $m = 0.8$. For acids: $K = 0.125$, $x = 0.50$, $y = -1.5$, $z = 1.85$, $m = 11/9$. For other families: $K = 0.158$, $x = 0.50$, $y = -1.50$, $z = 1.85$, $m = 11/9$. Some application examples of the previous expression can be found in Poling *et al.*[13]

In addition to the previous correlations, Miqueu *et al.*,[135] have proposed the following expression:

$$\gamma = k_B T_c \left(\frac{N_{av}}{V_c}\right) (4.35 + 4.14\omega)\, t^{1.26} \left(1 + 0.19 t^{0.5} + 0.25 t\right) \tag{30}$$

In Equation (30), V_c is the critical volume of the fluid and $t = 1 - T/T_c$. This correlation has been successfully applied for petroleum fluids (*i.e.* light gases, saturated hydrocarbons, aromatics) and polar compounds (*i.e.* refrigerants).

Interfacial Properties for Industrial Fluids

In this section, we test the proposed correlation for the case of industrial fluids. It is important to note that the approach used here is able to only to calculate the variation of the interfacial tension to the temperature but also to calculate the interfacial density profiles. As an example, we retake the model for hexane discussed in detail in Ref.[106]. Hexane is modelled in a coarse-grained fashion as a dimer, $m_s = 2$, and following the M & M procedure described in Ref.[106], an exponent of $\lambda = 19.26$ is obtained. Use of Equation (22) prescribes a value of $\alpha = 0.669$. Further use of the correlations in Ref.[106] yield $\varepsilon/k_B = 376.35$ K and $\sigma = 4.508$Å. With these data Equation (23) produces a value of $c = 36.182 \times 10^{-20}\,\mathrm{J}\,m^5\,\mathrm{mol}^{-2}$ The predicted results for phase equilibria, density profiles and surface tension are shown in Figures 4(a)-(d). Specifically, Figures 4(a)-(b) show the phase equilibrium in $\rho - T$ and $T - P$ projections, respectively. In these Figures we have included SAFT-VR Mie predictions, Molecular Dynamics results employing the same potentail ($\lambda = 19.26$,$\varepsilon/k_B = 376.35$ K and $\sigma = 4.508$ Å) and recommended experimental data from DECHEMA[136] and Figures 4(c)-(d) display the interfacial properties calculated from SAFT-VR Mie + SGT and the proposed expression for the influence parameter (see Equation (23)) and MD simulations carried out by using the same Mie parameters than the theory. From Figure 4(c), it is seen that these profiles display the expected behavior, (*i.e.*, they decrease monotonically across the interface following s hyperbolic tangent shape, that spans from the liquid to the vapor bulk phase). Noticeably there is a very good agreement between theory and simulations over a broad temperature range. Figure 4(d) represents the interfacial tension behavior as a function of temperature. From the latter figures, it is evident that here is a remarkable quantitative agreement to the MD results as well as to experimental tensiometry results all the way from low temperatures to the critical temperature. In the Supporting Information, we include a workbook written in Mathematica code that performs all calculations described above of

n-hexane.

In order to evaluate the performance of SAFT-VR Mie + SGT and the new expression for the influence parameter (see Equation (23)), we selected some test fluids (e.g. hydrocarbons, N_2, refrigerants, etc.), and applied a two-step predictive approach. First, the fluids are idealized as chains of CG tangential spheres interacting with each other through a Mie $(\lambda - 6)$ potential, whose parameters $(m_s, \varepsilon, \sigma, \lambda)$ are obtained by using the corresponding state principia described by Mejía *et al.*[106]. Basically, in this step once the number of beads in the chain is defined (m_s) by examining the overall molecular geometry (i.e. its length to beadth ratio), the value of λ is calculated from the acentric factor of the fluid (ω), expressing the relationship between the range of the potential and the vapor pressure of the fluid. In an analogous fashion, the energy parameter (ε) is obtained from the critical temperature of the fluid (T_c), and the value of σ is calculated from the liquid density evaluated at 0.7 of T_c. Once the Mie $(\lambda - 6)$ parameters have been identified, the van der Waals constant, α, can be computed from Equation (22) and the influence parameter is obtained from Equation (23). A second final step is to calculate the phase equilibrium from Equations (9) to (11) and the corresponding interfacial tension from Equation (5).

Table I summarizes the Mie $\lambda - 6$ parameters for an unabridged selection of fluids, taken from Ref.[106], and Figures 5(a)-(b) displays the variation of the interfacial tension with temperature for these selected fluids. These Figures include also the experimental tensiometry data reported by The Dechema data base.[136] Figure 5(a) displays the very good agreement with experimental data obtained from the theory. In fact, the overall Average Absolute Deviation (%AAD γ) of the calculated interfacial tensions is 2.8 % in the case of hydrocarbons (see Figure 5(a)), and 3.7 % for the other fluids selected (see Figure 5(b)).

In order to evaluate the performance of the proposed methodology to other correlations, table II includes the Average Absolute Deviation for the interfacial tension (%AAD γ) obtained from this work (*i.e.*, from Equation (5) and (23) and those calculated from correlations based on the corresponding state principia. Specifically, table II summarizes the %AAD γ obtained from the correlations developed by Brock and Bird[129], Curl and Pitzer[130], Zuo and Stenby[131], Sastri and Rao[132] and Miqueu *et al.*,[135]. It is seen that the proposed method is not only more accurate than other available correlations, but it is also broader in terms of applicability range.

CONCLUDING REMARKS

Several correlations exist which, based on semi-empirical corresponding states principia or otherwise, allow the calculation of interfacial tension of industrially relevant fluids. However, their application is typically restricted to the chemical family used to fix the constants involved. In this work we combine a molecular thermodynamic theory and molecular simulations in order to obtain faithful description of the tensiometry of molecular models of fluids and a mapping of it to experimental data. Specifically, this work combines a theoretical approach based on the SAFT-VR Mie EoS with the Square Gradient Theory (SGT) and Molecular Dynamics (MD). This approach is based on the description of the interfacial properties for short flexible chains composed of 2, 3, 4, 5 and 6 freely-jointed tangent spheres through a Mie $\lambda - 6$ ($\lambda = 8, 10, 12, 20$) potential. From the MD results, a simple, flexible and accurate expression for the correlation of the influence parameter in SGT is obtained. This expression provides a route to calculate the influence parameters for pure chain fluids by only using the molecular characteristics of the model fluid ($(m_s, \varepsilon, \sigma, \lambda)$). By combining this approach with previous mappings of the Mie potential to pure fluids (Ref.[106]) one can effectively predict the bulk and interfacial properties of pure fluids from the knowledge of only three widely available properties: the critical temperature, the accentric factor, and a liquid density. A key aspect of the methodology is the internal consistency of the molecular model, i.e. both the theory and the simulations are based on the same set of unique force field descriptors. The correlation for the influence parameter can be used for describing molecular coarse grained fluids with an absolute deviation lower than 2.02%.

Uniquely, the procedure could also be inverted: given the interfacial tension of a fluid, a set of Mie parameters can be specifically found by a simple analytical approach without the need of performing simulations. This is particularly useful in developing top-down coarse-grain potential for simulations of surfactants and interfacial fluids. This extension is not pursued here but will be the subject of future work.

The proposed molecular model is both robust and transferable, producing both as set of molecular parameters amenable to be used in molecular simulation and a fully consistent theory for predicting the interfacial properties of Mie fluids. It is applicable in as much as a homonuclear non-associating chain remains a good model of the pure fluid; i.e. if is not expected to work for strongly associating fluids (e.g. water and small alcohols). However,

where applicable, the predictions show a remarkable accuracy when compared to traditional corresponding state principa correlations. In addition, the proposed approach not only gives an excellent model to predict the interfacial tension over a wide temperature range, even very close to the critical region, but also provides a route to obtain microscopic information of the interfacial region, such as interfacial density profiles.

ACKNOWLEDGMENTS

This paper is dedicated to the memory of Prof. Hugo Segura (1965-2014). Hugo was not only an excellent researcher and tutor but actually an academic father for many of us. He truly had an amazing physical intuition and understanding of the complex mechanisms underlying fluid phase and interfacial behavior. J. M. G. acknowledges the doctoral scholarship from Conicyt (Chile) and from Red Doctoral REDOC.CTA, MINEDUC project UCO1202 at U. de Concepción. A. M acknowledges the financial support from FONDECYT (Chile) under the Project 1150656. E. A. M. acknowledges support from the U.K. Engineering and Physical Sciences Research Council (EPSRC) through research grants to the Molecular Systems Engineering group (Grants EP/ E016340, and EP/J014958). M. M. P. acknowledges CESGA (www.cesga.es) for providing access to computing facilities, and Ministerio de Economía y Competitividad, (Proj. Refs. FIS2012-33621 and FIS2015-68910-P, cofinanced with EU FEDER funds). F. J. B. also acknowledges Ministerio de Economía y Competitividad (Proj. Ref. FIS2013-46920-C2-1-P, cofinanced with EU FEDER funds). Additional funding from Junta de Andalucía and Universidad de Huelva is also acknowledged.

SUPPORTING INFORMATION AVAILABLE

Supplementary data associated with this article can be found in the online version. We include the numerical values of the slopes for Mie $\lambda - 6$ fluids as a function of λ. (see table S. I), and the Molecular Dynamics simulation (see table S. II) raw results of interfacial tensions for short flexible chains composed of 2, 3, 4, 5 and 6 freely-jointed tangent spheres interacting through a Mie $(\lambda - 6)$ $(\lambda = 8, 10, 12, 20)$. We also include a general Mathematica code (SAFT-VR Mie + SGT) to predict the phase and interfacial behavior of fluids using as input either critical properties or Mie potential parameters.

LITERATURE CITED

[1] Rowlinson JS, Widom B. *Molecular Theory of Capillarity.* Clarendon, Oxford. 1982.

[2] Debenedetti PG. *Metastable Liquids, Concepts and Principles.* Princeton University Press, Princeton. 1996.

[3] Evans MJB. *Measurement of surface and interfacial tension.* Elsevier. 2006.

[4] Frenkel D, Smit B. *Understanding Molecular Simulation.* Academic Press, New York. 2002.

[5] Davis HT, Scriven LE. Stress and Structure in Fluid Interfaces. *Adv Chem Phys.* 1982; 49:357–454.

[6] Gray CG, Gubbins KE, Joslin CG. *Theory of Molecular Fluids. Volume 2: Applications.* Oxford University Press. 2011.

[7] Rusanov AI, Prokhorov VA. *Interfacial Tensiometry.* Elsevier. 1996.

[8] Holcomb CD, Clancy P, Zollweg JA. A critical study of the simulation of the liquid-vapour interface of a Lennard-Jones fluid. *Mol Phys.* 1993;78(2):437–459.

[9] Hulshof H. The Direct Deduction of the Capillarity Constant as a Surface Tension. *Ann Phys.* 1901;4:165–186.

[10] Irving JH, Kirkwood JG. The Statistical Mechanical Theory of Transport Processes. IV. The Equations of Hydrodynamics. *J Chem Phys.* 1950;18(6):817–829.

[11] Gloor GJ, Jackson G, Blas FJ, de Miguel E. Test-area simulation method for the direct determination of the interfacial tension of systems with continuous or discontinuous potentials. *J Chem Phys.* 2005;123(13):134703–134721.

[12] Macleod DB. On a relation between surface tension and density. *Trans Faraday Soc.* 1923; 19:38–41.

[13] Poling BE, Prausnitz JM, O'Connell JP. *The Properties of Gases and Liquids.* McGraw-Hill , New York. 2000.

[14] Guggenheim EA. The Principle of Corresponding States. *J Chem Phys.* 1946;13(253–261).

[15] Xiang HW. *The Corresponding-States Principle and its Practice: Ther- modynamic, Transport and Surface Properties of Fluids.* Elsevier, Amsterdam. 2005.

[16] van der Waals JD. The thermodynamik theory of capillarity under the hypothesis of a continuous variation of density. *Zeit Phys Chem.* 1894;13:675–725.

[17] Rowlinson JS. Translation of J. D. van der Waals' "The thermodynamik theory of capillarity under the hypothesis of a continuous variation of density". *J Statist Phys.* 1979;20(2):197–200.

[18] Wu J, Li Z. Density-Functional Theory for Complex Fluids. *Annu Rev Phys Chem.* 2007; 58:85–112.

[19] Llovell F, Galindo A, Blas FJ, Jackson G. Classical density functional theory for the prediction of the surface tension and interfacial properties of fluids mixtures of chain molecules based on the statistical associating fluid theory for potentials of variable range. *J Chem Phys.* 2010;133:024704.

[20] Fu D, Wu J. Vapor-liquid equilibria and interfacial tensions of associating fluids within a density functional theory. *Ind Eng Chem Res.* 2005;44:1120–1128.

[21] Fu D, Wu J. A self-consistent approach for modeling the interfacial properties and phase diagrams of Yukawa, Lennard-Jones and square-well fluids. *Mol Phys.* 2004;102(13):1479–1488.

[22] Carey BS, Scriven LE, Davis HT. Semiempirical theory of surface tensions of pure normal alkanes and alcohols. *AIChE J.* 1978;24(6):1076–1080.

[23] Carey BS, Scriven LE. Semiempirical theory of surface tension of binary systems. *AIChE J.* 1980;26(5):705–711.

[24] Sahimi M, Taylor BN. Surface tension of binary liquid vapor mixtures. A comparison of mean field and scaling theories. *J Chem Phys.* 1991;95(9):6749–6761.

[25] Cornelisse PMW, Peters CJ, de Swaan Arons J. Application of the Peng-Robinson equation of state to calculate interfacial tensions and profiles at vapour-liquid interfaces. *Fluid Phase Equilib.* 1993;82:119–129.

[26] Cornelisse PMW, Peters CJ, de Swaan Arons J. Simultaneous prediction of phase equilibria, interfacial tension and concentration profiles. *Mol Phys.* 1993;80(4):941–955.

[27] Zuo YX, Stenby EH. Calculation of interfacial tensions with gradient theory. *Fluid Phase Equilib.* 1997;132(1):139–158.

[28] Carey VP. Thermodynamic properties and structure of the liquid-vapor interface: A neoclassical Redlich-Kwong model. *J Chem Phys.* 2003;118(11):5053–5064.

[29] Miqueu C, Mendiboure B, Graciaa A, Lachaise J. Modelling of the surface tension of pure components with the gradient theory of fluid interfaces. a simple and accurate expression for the influence parameters. *Fluid Phase Equilib.* 2003;207(1-2):225–246.

[30] Miqueu C, Mendiboure B, Graciaa A, Lachaise J. Modelling of the surface tension of binary and ternary mixtures with the gradient theory of fluid interfaces. *Fluid Phase Equilib.* 2004; 218:189–203.

[31] Mejía A, Segura H. Interfacial behavior in Type IV systems. *Int J Thermophys.* 2004; 25(5):1395–1414.

[32] Mejía A, Segura H. On the interfacial behavior about the shield region. *Int J Thermophys.* 2005;26(1):13–29.

[33] Miqueu C, Mendiboure B, Graciaa A, Lachaise J. Modeling of the Surface Tension of Multicomponent Mixtures with the Gradient Theory of Fluid Interfaces. *Ind Eng Chem Res.* 2005;44:3321–3329.

[34] Lin H, Duan YY, Min Q. Gradient theory modeling of surface tension for pure fluids and binary mixtures. *Fluid Phase Equilib.* 2007;254(1-2):75–90.

[35] Miqueu C, Mendiboure B, Graciaa A, Lachaise J. Petroleum mixtures: An efficient predictive method for surface tension estimations at reservoir conditions. *Fuel.* 2008;87(6):612–621.

[36] Mejía A, Segura H, Vega LF, Wisniak J. Simultaneous prediction of interfacial tension and phase equilibria in binary mixtures. An approach based on cubic equations of state with improved mixing rules. *Fluid Phase Equilib.* 2005;227:225–238.

[37] Mejía A, Segura H, Wisniak J, Polishuk I. Correlation and prediction of interface tension for fluid mixtures: An approach based on cubic equations of state with the wong-sandler mixing rule. *J Phase Equilib Diffus.* 2005;26(3):215–224.

[38] Cornelisse PMW, Wijtkamp M, Peters CJ. Interfacial tensions of fluid mixtures with polar and associating components. *Fluid Phase Equilib.* 1998;150–151:633–640.

[39] Queimada AJ, Miqueu C, Marrucho IM, Kontogeorgis GM, Coutnho JAP. Modeling vapor-liquid interfaces with the gradient theory in combination with the CPA equation of state. *Fluid Phase Equilib.* 2005;228–229:479–485.

[40] Kalikmanov VI. *Statistical Physics of Fluids, Basic Concepts, and Applications.* Springer, New York. 2011.

[41] Mejía A, Polishuk I, Segura H, Wisniak J. Estimation of interfacial behavior using the global phase diagram approach: I. Carbon dioxide-n-alkanes. *Thermochim Acta*. 2004;411(2):171–176.

[42] Dhams RN. Gradient Theory simulations of pure fluid interfaces using a generalized expression for influence parameters and a Helmholtz energy equation of state for fundamentally consistent two-phase calculations. *J Colloid Interface Sci*. 2014;445:48–59.

[43] Poser CI, Sanchez IC. Surface tension theory of pure liquids and polymer melts. *J Colloid Interface Sci*. 1979;69(3):539–548.

[44] Poser CI, Sanchez IC. Interfacial tension theory of low and high molecular weight liquid mixtures. *Macromolecules*. 1981;14(2):361–370.

[45] Kahl H, Enders S. Calculation of surface properties of pure fluids using density gradient theory and SAFT-EOS. *Fluid Phase Equilib*. 2000;172(1):27–42.

[46] Kahl H, Enders S. Interfacial properties of binary mixtures. *Phys Chem Chem Phys*. 2002; 4:931–936.

[47] Panayiotou C. Interfacial Tension and Interfacial Profiles of Fluids and Their Mixtures. *Langmiur*. 2002;18:8841–8853.

[48] Duque D, Pàmies JC, Vega LF. Interfacial properties of Lennard-Jones chains by direct simulation and density gradient theory. *J Chem Phys*. 2004;121(22):11395–11401.

[49] Mejía A, Pàmies JC, Duque D, Segura H, Vega LF. Phase and interface behaviors in type-I and type-V Lennard-Jones mixtures: Theory and simulations. *J Chem Phys*. 2005; 123(3):034505–034514.

[50] Mejía A, Segura H, Wisniak J, Polishuk I. Association and molecular chain length effects on interfacial behaviour. *Phys Chem Liq*. 2006;44(1):45–59.

[51] Mejía A, Vega LF. Perfect Wetting along a Three-Phase Line: Theory and Molecular Dynamics Simulations. *J Chem Phys*. 2006;124(24):244505–244512.

[52] Li XS, Liu JM, Fu D. Investigation of Interfacial Tensions for Carbon Dioxide Aqueous Solutions by Perturbed-Chain Statistical Associating Fluid Theory Combined with Density-Gradient Theory. *Ind Eng Chem Res*. 2008;47:8911–8917.

[53] Galliero G, Piñeiro MM, Mendiboure B, Miqueu C, Lafitte T, Bessières D. Interfacial properties of the Mie n-6 fluid: Molecular simulations and gradient theory results. *J Chem Phys*. 2009;130(10):104704–104713.

[54] Müller EA, Mejía A. Interfacial properties of selected binary mixtures containing n-alkanes. *Fluid Phase Equilib.* 2009;282(2):68–81.

[55] Fu D, Jiang H, Wang B, Fu S. Investigation of the surface tension of methane and n-alkane mixtures by perturbed-chain statistical associating fluid theory combined with density-gradient theory. *Fluid Phase Equilib.* 2009;279(2):136–140.

[56] Lafitte T, Mendiboure B, Piñeiro MM, Bessières D, Miqueu C. Interfacial properties of water/CO_2: a comprehensive description through a gradient theory-SAFT-VR Mie approach. *J Phys Chem B.* 2010;114(34):11110–11116.

[57] Müller EA, Mejía A. Comparison of United-Atom Potentials for the Simulation of Vapor-Liquid Equilibria and Interfacial Properties of Long-Chain n-Alkanes up to n-C_{100}. *J Phys Chem B.* 2011;115(44):12822–12834.

[58] Miqueu C, Míguez JM, Piñeiro MM, Lafitte T, Mendiboure B. Simultaneous Application of the Gradient Theory and Monte Carlo Molecular Simulation for the Investigation of Methane/Water Interfacial Properties. *J Phys Chem B.* 2011;115(31):9618–9625.

[59] Niño-Amézquita G. Phase equilibrium and interfacial properties of water + CO2 mixtures. *Fluid Phase Equilib.* 2012;332:40–47.

[60] Khosharay S, Mazraeno MS, Varaminian F. Modeling the surface tension of refrigerant mixtures with linear gradient theory. *Int J Ref.* 2013;36:2223–2232.

[61] Khosharay S, Varaminian F. Modeling interfacial tension of (CH_4+N_2)+H_2O and (N_2+CO_2)+H_2O systems using linear gradient theory. *Koren J Chem Eng.* 2013;30(3):724–732.

[62] Khosharay S, Mazraeno MS, Varaminian F, Bagheri A. A proposed combination model for predicting surface tension and surface properties of binary refrigerant mixtures. *Int J Ref.* 2014;40:347–361.

[63] Khosharay S, Abolala M, Varaminian F. Modeling the surface tension and surface properties of (CO_2 + H_2O) and (H_2S + H_2O) with gradient theory in combination with sPC-SAFT EOS and a new proposed influence parameter. *J Mol Liq.* 2014;198:292–298.

[64] Schäfer E, Horbach F, Enders S. Modeling of Liquid–Liquid Interfacial Properties of Binary and Ternary Mixtures. *J Chem Eng Data.* 2014;59(10):3003–3016.

[65] Míguez JM, Garrido JM, Blas FJ, Segura H, Mejía A, Piñeiro MM. Comprehensive Characterization of Interfacial Behavior for the Mixture CO_2+H_2O+CH_4: Comparison between

Atomistic and Coarse Grained Molecular Simulation Models and Density Gradient Theory. *J Phys Chem C*. 2014;118(42):24504–24519.

[66] Cumicheo C, Cartes M, Müller EA, Mejía A. High-pressure densities and interfacial tensions of binary systems containing carbon dioxide + n-alkanes: (n-Dodecane, n-tridecane, n-tetradecane). *Fluid Phase Equilib*. 2014;380:82–92.

[67] Mejía A, Cartes M, Segura H, Müller EA. Use of Equations of State and Coarse Grained Simulations to Complement Experiments: Describing the Interfacial Properties of Carbon Dioxide + Decane and Carbon Dioxide + Eicosane Mixtures. *J Chem Eng Data*. 2014; 50(10):2928–2941.

[68] Garrido JM, Quinteros-Lama H, Piñeiro MM, Mejía A, Segura H. On the phase and interface behavior along the three-phase line of ternary Lennard-Jones mixtures: A collaborative approach based on square gradient theory and molecular dynamics simulations. *J Chem Phys*. 2014;141(1):014503–014514.

[69] Schäfer E, Sadowski G, Enders S. Interfacial tension of binary mixtures exhibiting azeotropic behavior: Measurement and modeling with PCP-SAFT combined with Density Gradient Theory. *Fluid Phase Equilib*. 2014;362:151–162.

[70] Grunert T, Enders S. Prediction of interfacial properties of the ternary system water + benzene + butan-1-ol. *Fluid Phase Equilib*. 2014;381:46–50.

[71] Chow YF, Eriksen DK, Galindo A, Haslam AJ, Jackson G, Maitland GC, Martin JP. Interfacial tensions of systems comprising water, carbon dioxide and diluent gases at high pressures: Experimental measurements and modelling with SAFT-VR Mie and square-gradient theory. *Fluid Phase Equilib*. 2016;407:159–176.

[72] Baidavok VG, Protsenko SP, Chernykh GG, Boltachev GS. Statistical substantiation of the van der Waals theory of inhomogeneous fluids. *Phys Rev E*. 2002;65(4):041601–041616.

[73] Bongiorno V, Scriven LE, Davis HT. Molecular theory of fluid interfaces. *J Colloid Interface Sci*. 1976;57(3):462–475.

[74] Bongiorno V, Davis HT. Modified Van der Waals theory of fluid interfaces. *Phys Rev A*. 1975;12(5):2213–2224.

[75] Breure B, Peters CJ. Modeling of the surface tension of pure components and mixtures using the density gradient theory combined with a theoretically derived influence parameter correlation. *Fluid Phase Equilib*. 2012;334:189–196.

[76] Carey BS. The gradient theory of fluid interfaces. Ph.D. thesis, University of Minnesota. 1979.

[77] Peng DY, Robinson DB. A New Two-Constant Equation of State. *Ind Eng Chem Fundam.* 1976;15(1):59–64.

[78] Vilaseca O, Vega LF. Direct calculation of interfacial properties of fluids close to the critical region by a molecular-based equation of state. *Fluid Phase Equilib.* 2011;306(1):4–14.

[79] Lafitte T, Apostolakou A, Avendaño C, Galindo A, Adjiman CS, Müller EA, Jackson G. Accurate statistical associating fluid theory for chain molecules formed from Mie segments. *J Chem Phys.* 2013;139(15):154504–154540.

[80] Papaioannou V, Lafitte T, Avendaño C, Adjiman CS, G Jackson EAM, Galindo A. Group contribution methodology based on the statistical associating fluid theory for heteronuclear molecules formed from Mie segments. *J Chem Phys.* 2014;140:054107.

[81] Avendaño C, Lafitte T, Galindo A, Adjiman CS, Jackson G, Müller EA. SAFT-γ Force Field for the Simulation of Molecular Fluids. 1. A Single-Site Coarse Grained Model of Carbon Dioxide. *J Phys Chem B.* 2011;115(38):11154–11169.

[82] Avendaño C, Lafitte T, Adjiman CS, Galindo A, Müller EA, Jackson G. SAFT-γ Force Field for the Simulation of Molecular Fluids: 2. Coarse-Grained Models of Greenhouse Gases, Refrigerants, and Long Alkanes. *J Phys Chem B.* 2013;117(9):2717–2733.

[83] Lafitte T, Avendaño C, Papaionnou V, Galindo A, Adjiman CS, Jackson G, Müller EA. SAFT-γ force field for the simulation of molecular fluids: 3. Coarse-grained models of benzene and hetero-group models of n-decylbenzene. *Mol Phys.* 2012;110(11–12):1189–1203.

[84] Müller EA, Jackson G. Force-Field Parameters from the SAFT-gamma Equation of State for Use in Coarse-Grained Molecular Simulations. *Ann Rev Chem Biomol Eng.* 2014;5(1):405–427.

[85] Lobanova O, Lafitte T, Avendaño C, Müller EA, Jackson G. SAFT-γ Force Field for the Simulation of Molecular Fluids: 4. A single-site coarse-grained model of water applicable over a wide temperature range. *Mol Phys.* 2015;113:1228–1249.

[86] Herdes C, Totton TS, Müller EA. Coarse grained force field for the molecular simulation of natural gases and condensates. *Fluid Phase Equilib.* 2015;406:91–100.

[87] Lobanova O, Mejía A, Jackson G, Müller EA. SAFT-γ force field for the simulation of molecular fluids 6: Binary and ternary mixtures comprising water, carbon dioxide, and n-

alkanes. *J Chem Thermodynamics*. 2016;93:320–336.

[88] de Vries EC. Metingen over den invloed van de temperatuur op de capillaire stijghoogte bij aether, tussen den kritischen toestand en het kookpunt van aethyleen. *Versl Kon Akad*. 1892; 1(156–158).

[89] Kipnes AY, Yavelov BE, Rowlinson JS. *Van der Waals and Molecular Science*. Oxford University Press, New York. 1996.

[90] Sengers JL. *How Fluids Unmix: Discoveries by the School of Van der Waals and Kamerlingh Onnes*. History of Science and Scholarship in the Netherlands. 2003.

[91] Rowlinson JS. *Cohesion: A Scientific History of Intermolecular Forces*. Cambridge University Press. 2005.

[92] Cahn JW, Hilliard JE. Free Energy of a Nonuniform System. I- Interfacial Free Energy. *J Chem Phys*. 1958;28(2):258–267.

[93] Yang AJM, Fleming PD, Gibbs JH. Molecular theory of surface tension. *J Chem Phys*. 1976; 64(9):3732–3747.

[94] Yang AJM. Molecular theory of surface tension. Ph.D. thesis, Brown University. 1975.

[95] Poser CI. Interfacial tension theory for low molecular weight and polymer systems. Ph.D. thesis, University of Massachusetts. 1980.

[96] Cornelisse PMW. The squared gradient theory applied. Simultaneous modelling of interfacial tension and phase behaviour. Ph.D. thesis, Delft University. 1997.

[97] Miqueu C. Modélisation, à température et pression élevées, de la tension superficielle de composants des fluides pétroliers et de leurs mélanges synthétiques ou réels. Ph.D. thesis, Université de Pau et des Pays de l'Adour. 2001.

[98] Mejía A. Comportamiento Interfacial de Mezclas Fluidas en Equilibrio. Ph.D. thesis, Universidad de Concepción. 2004.

[99] Davis HT, Scriven LE, Prigoginen I, Rice SA. Stress and structure in fluid interfaces. *Adv Chem Phys*. 1982;48(357–454).

[100] Davis HT. *Statistical Mechanics of Phases, Interfaces and Thin Films*. Wiley. 1996.

[101] McCabe C, Galindo A. SAFT Associating fluids and fluid mixtures. In: *Applied Thermodynamics of Fluids*, edited by Goodwin A, Sengers JV, Peters CJ, chap. 8. Royal Society of Chemistry, London. 2010;.

[102] Müller EA, Gubbins KE. Molecular-based equations of state for associating fluids: A review of SAFT and related approaches. *Ind Eng Chem Res*. 2001;10:2193–2211.

[103] Mie G. Zur Kinetischen Theorie der Einatomigen Körper. *Ann Phys*. 1903;316:657–697.

[104] Jones JE. On the Determination of Molecular Fields. II. From the Equation of State of a Gas. *Proc R Soc A*. 1924;106(738):463–477.

[105] Jorgensen WL, Madura JD, Swenson CJ. Optimized Intermolecular Potential Functions for Liquid Hydrocarbons. *J Am Chem Soc*. 1984;106:6638–6646.

[106] Mejía A, Herdes C, Müller EA. Force Fields for Coarse-Grained Molecular Simulations from a Corresponding States Correlation. *Ind Eng Chem Res*. 2014;53(10):4131–4141.

[107] Ramrattan NS, Avendaño C, Müller EA, Galindo A. A corresponding-states framework for the description of the Mie family of intermolecular potentials. *Mol Phys*. 2015;113:932–947.

[108] Eisenschitz R, London F. Über das Verhältnis der van der Waalsschen Kräfte zu den homöopolaren Bindungskräften. *Zeitschrift für Physik*. 1930;60((7-8)):491–527.

[109] Percus JK, Yevick GJ. Hard-Core Insertion in the Many-Body Problem. *Phys Rev*. 1964; 136:B290–B296.

[110] Tardón MJ, Garrido JM, Quinteros-Lama H, Mejía A, Segura H. Molar isopycnicity in heterogeneous binary mixtures. *Fluid Phase Equilib*. 2012;336:84–97.

[111] Sutherland W. The viscosity of gases and molecular force. *Philos Mag*. 1893;36(223):507–531.

[112] Allen MP, Tildesley DJ. *Computer Simulation of Liquids*. Oxford University Press, New York. 1987.

[113] Martínez-Veracoechea F, Müller EA. Temperature-quench Molecular Dynamics Simulations for Fluid Phase Equilibria. *Mol Simul*. 2005;31(1):33–43.

[114] Galliero G. Surface tension of short flexible Lennard-Jones chains: Corresponding states behavior. *J Chem Phys*. 2010;133(7):074705–074710.

[115] Míguez JM, Piñeiro MM, Blas FJ. Influence of the Long-Range Corrections on the Interfacial Properties of Molecular Models Using Monte Carlo Simulation. *J Chem Phys*. 2012; 138(3):034707–034716.

[116] Cuendet MA, van Gunsteren WF. On the calculation of velocity-dependent properties in molecular dynamics simulations using the leapfrog integration algorithm. *J Chem Phys*. 2007;127(18):184102–184109.

[117] Nosé S. A molecular dynamics method for simulations in the canonical ensemble. *Mol Phys.* 1984;52(2):255–268.

[118] Hoover WG. Canonical dynamics: Equilibrium phase-space distributions. *Phys Rev A.* 1985; 31:1695–1697.

[119] Berendsen HJC, Postma JPM, van Gunsteren WF, di Nola A, Haak JR. Molecular dynamics with coupling to an external bath. *J Chem Phys.* 1984;81(8):3684–3690.

[120] Duque D, Vega LF. Some issues on the calculation of interfacial properties by molecular simulation. *J Chem Phys.* 2004;121(17):8611–8617.

[121] Blas FJ, MacDowell LG, de Miguel E, Jackson G. Vapor-liquid interfacial properties of fully flexible Lennard-Jones chains. *J Chem Phys.* 2008;129(14):144703–144711.

[122] Blas FJ, Bravo AIMV, Míguez JM, Piñeiro MM, MacDowell LG. Vapor-liquid interfacial properties of rigid-linear Lennard-Jones chains. *J Chem Phys.* 2012;137(8):084706–084716.

[123] Blas FJ, Martínez-Ruiz FJ, Bravo AIMV, MacDowell LG. Universal scaling behaviour of surface tension of molecular chains. *J Chem Phys.* 2012;137(2):024702–024706.

[124] Blas FJ, Bravo AIMV, Algaba J, Martínez-Ruiz FJ, MacDowell LG. Effect of molecular flexibility of Lennard-Jones chains on vapor-liquid interfacial properties. *J Chem Phys.* 2014; 140(11):114705–114715.

[125] Gil-Villegas A, Galindo A, Whitehead PJ, Mills SJ, Jackson G, Burgess AN. Statistical Associating Fluid Theory for Chain Molecules with Attractive Potentials of Variable Range. *J Chem Phys.* 1997;106:4168–0000.

[126] Lafitte T, Bessières D, Piñeiro MM, Daridon JL. Simultaneous estimation of phase behavior and second-derivative properties using the statistical associating fluid theory with variable range approach. *J Chem Phys.* 2006;124(2):024509–024524.

[127] Lafitte T, Piñeiro MM, Daridon JL, Bessières D. A Comprehensive Description of Chemical Association Effects on Second Derivative Properties of Alcohols through a SAFT-VR Approach. *J Phys Chem B.* 2007;111(13):3447–3461.

[128] Wu J. Density functional theory for liquid structure and thermodynamics. In: *Molecular Thermodynamics of Complex Systems*, edited by Lu X, Hu H, vol. 131 of *Structure and Bonding*, chap. 1, pp. 1–74. Springer, New York. 2009;.

[129] Brock JR, Bird RB. Surface Tension and the Principle of Corresponfing States. *AIChE J.* 1955;1(2):174–177.

[130] Curl RFJ, Pitzer KS. Volumetric and Thermodynamic Properties of Fluids-Enthalpy, Free Energy, and Entropy. *Ind Eng Chem*. 1958;50:265–274.

[131] Zuo YX, Stenby EH. Corresponding-States and Parachor Models for the Calculation of Interfacial Tensions. *Can J Chem Eng*. 1997;75:1130–1137.

[132] Sastri SRS, Rao KK. A simple method to predict surface tension of organic liquids. *J Chem Eng*. 1995;59:181–186.

[133] Riedel L. Eine neue universelle Dampfdruckformel Untersuchungen uber eine Erweiterung des Theorems der ubereinstimmenden Zustande. *Chem Ing Tech*. 1954;26:83–89.

[134] Miller DG. On the reduced Frost-Kalkwarf vapor pressure equation. *Ind Eng Chem Fundam*. 1963;2:78–79.

[135] Miqueu C, Broseta D, Satherley J, Mendiboure B, Lachaise J, Graciaa A. An extended scaled equation for the temperature dependence of the surface tension of pure compounds inferred from an analysis of experimental data. *Fluid Phase Equilib*. 2000;172:169–182.

[136] DECHEMA Gesellschaft für Chemische Technik und Biotechnologie e.V., Frankfurt am Main, Germany, https://cdsdt.dl.ac.uk/detherm/, (retrieved February, 2015).

FIGURES CAPTIONS

FIGURE 1

Relationship between reduced tensions calculated from MD (abscissa) and the results from SGT (c.f. eq. (20)). The slope of the curve is proportional to $\sqrt{c}/(m_s)$. (a) Mie (8-6), (b) Mie (10-6), (c) Mie (12-6), (d) Mie (20-6) molecular chains fluid. Mie λ-6 chains formed from $m_s = 1$ (circle), $m_s = 2$ (squares), $m_s = 3$ (diamonds), $m_s = 4$ (inverted triangles), $m_s = 5$ (triangles), $m_s = 6$ (right triangles) segments.

FIGURE 2

Density profiles across the vapour-liquid interface of flexible Mie 10-6 chains formed by (a) $m_s = 2$, (b) $m_s = 3$, (c) $m_s = 4$ and (d) $m_s = 5$. (Solid line) density profiles calculated with the SAFT-VR Mie + SGT and Equation (23) for the influence parameter, (stars) Density profiles obtained from MD simulations.

FIGURE 3

Interfacial tensions (γ^*) as a function of temperature (T^*) for molecular chain fluids with $m_s = 1$ to 6 interacting by a Mie $\lambda - 6$ potential. (a) Mie (8-6); (b) Mie (10-6); (c) Mie (12-6); (d) Mie (20-6). (Solid line) calculated with the SAFT-VR Mie + SGT and Equation (23) for the influence parameters. (dash dotted line) calculated with the LJ-Chains + SGT using the influence parameter proposed by Duque *et al.*[48]. Symbols as in Figure 1.

FIGURE 4

Phase equilibria and interfacial properties for n-hexane. (a) Coexistence densities ($\rho - T$ projection); (b) vapor pressure ($T - P$ projection); (c) density profile across the vapor-liquid interface ($\rho - z$ projection); (d). Interfacial tension ($\gamma - T$ projection). (Solid line) SAFT-VR Mie + SGT with the influence parameter calculated from Equation (23). (stars) density profiles obtained from MD simulations, (squares) results from MD simulations; (filled black circle) recomended experimental data from DECHEMA[136].

FIGURE 5

Comparison between calculated (lines) with the SAFT-VR Mie+SGT and Equation (23) for the influence parameters and experimental[136] (symbols) interfacial tensions as a function of temperature for various components. Information about the SAFT-VR Mie

parameters that were used in the calculations and the experimental data can be found in table II.

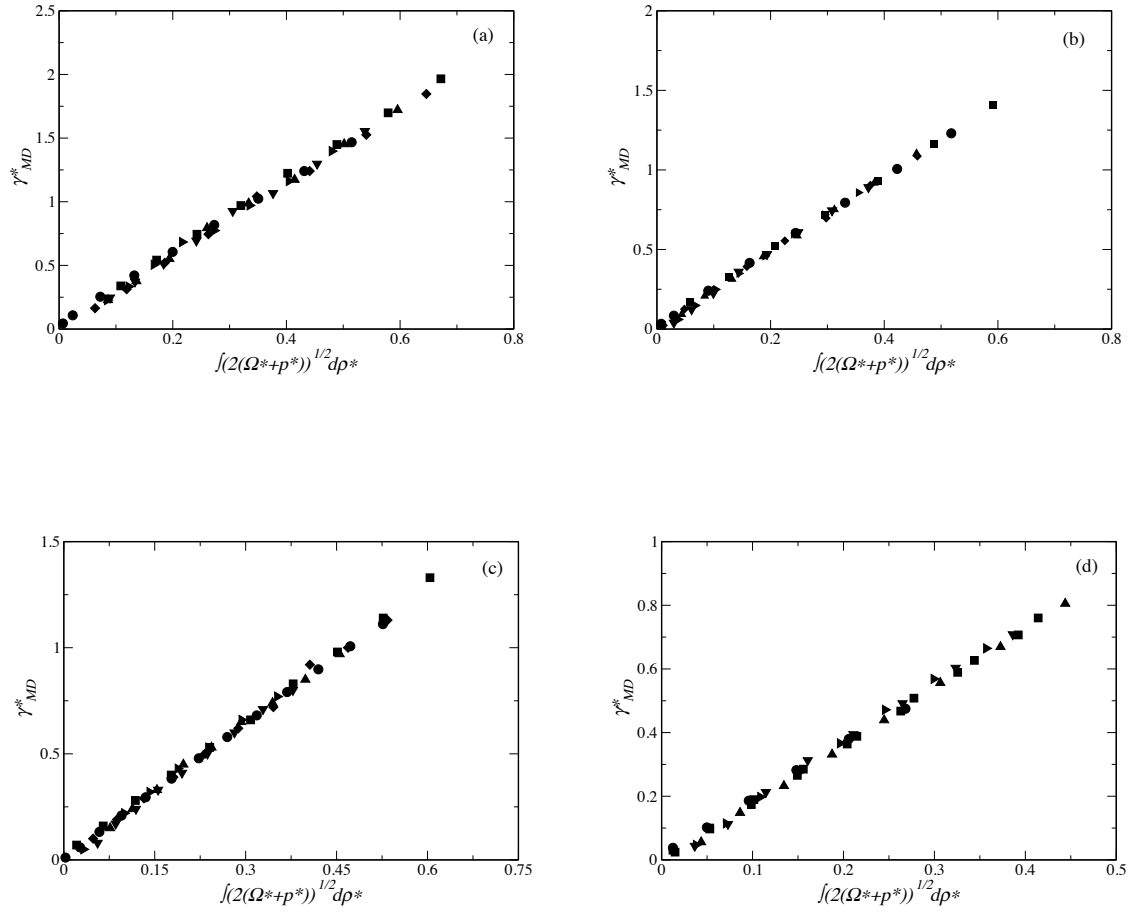

FIG. 1

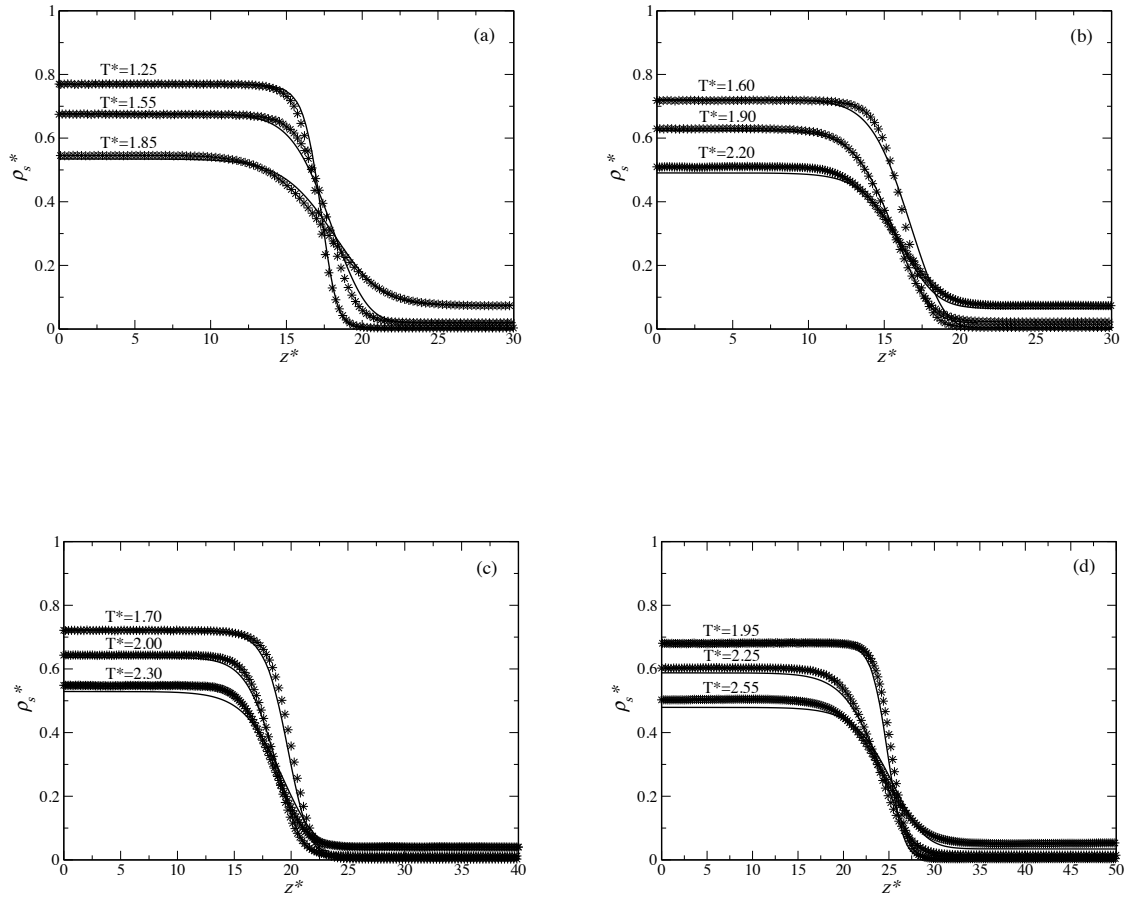
(a)
T*=1.25
T*=1.55
T*=1.85
(b)
T*=1.60
T*=1.90
T*=2.20
(c)
T*=1.70
T*=2.00
T*=2.30
(d)
T*=1.95
T*=2.25
T*=2.55
ρ_s^*
z^*

FIG. 2

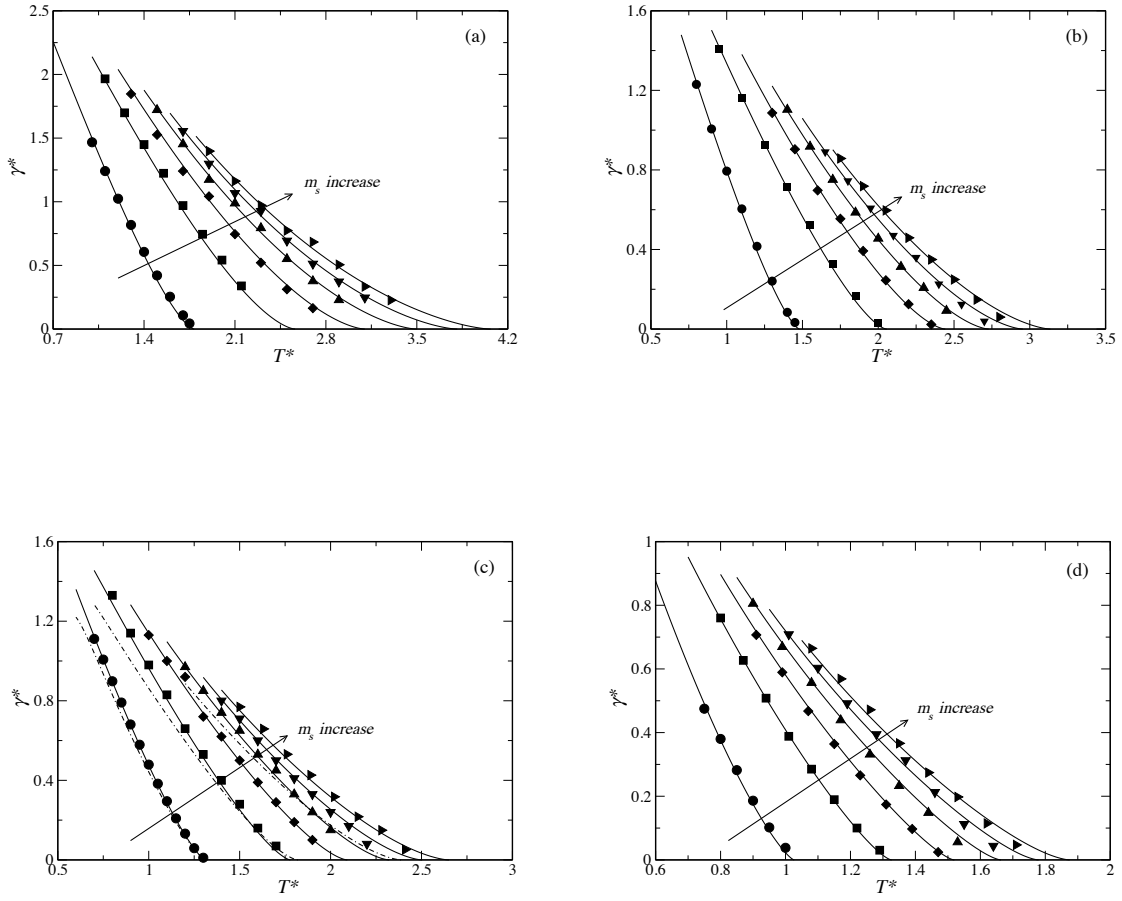

FIG. 3

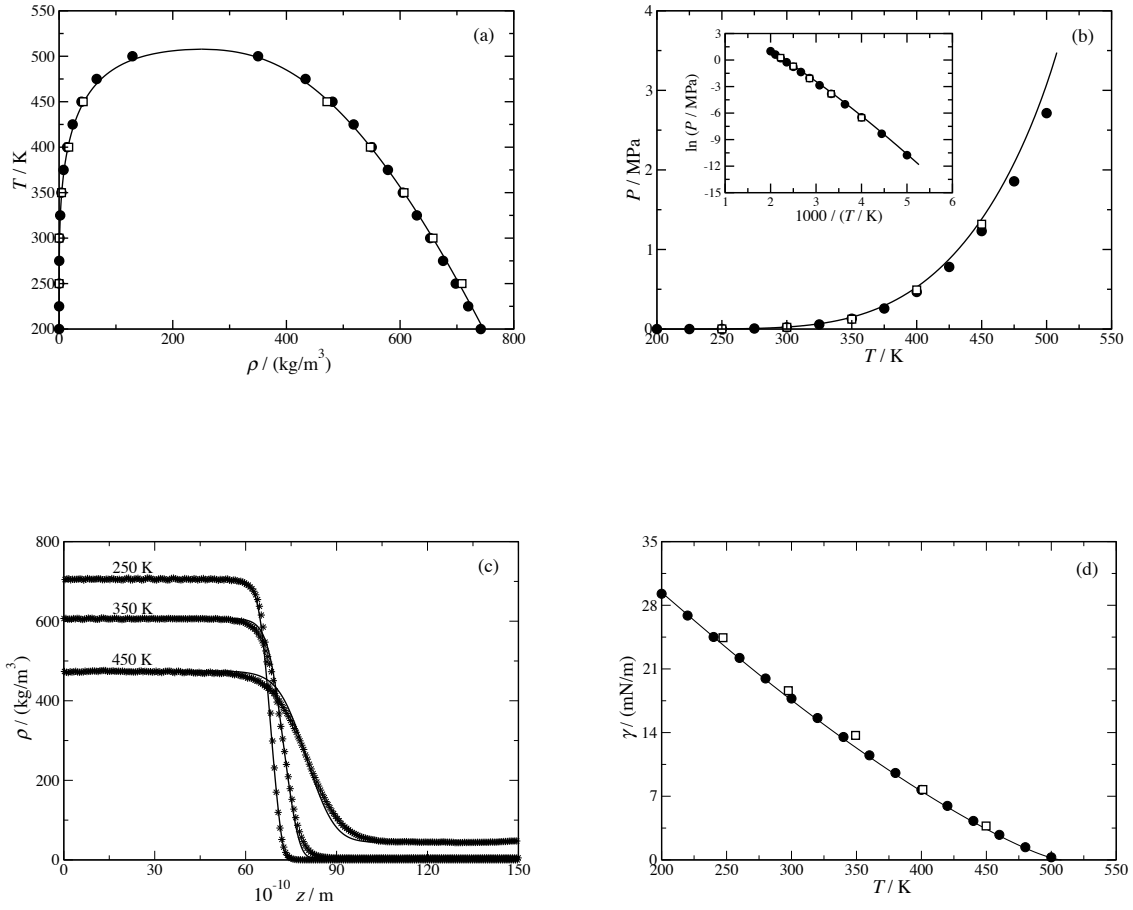
(a)
T / K
ρ / (kg/m3)
(b)
P / MPa
T / K
ln (P / MPa)
1000 / (T / K)
(c)
250 K
350 K
450 K
ρ / (kg/m3)
10-10 z / m
(d)
γ / (mN/m)
T / K

FIG. 4

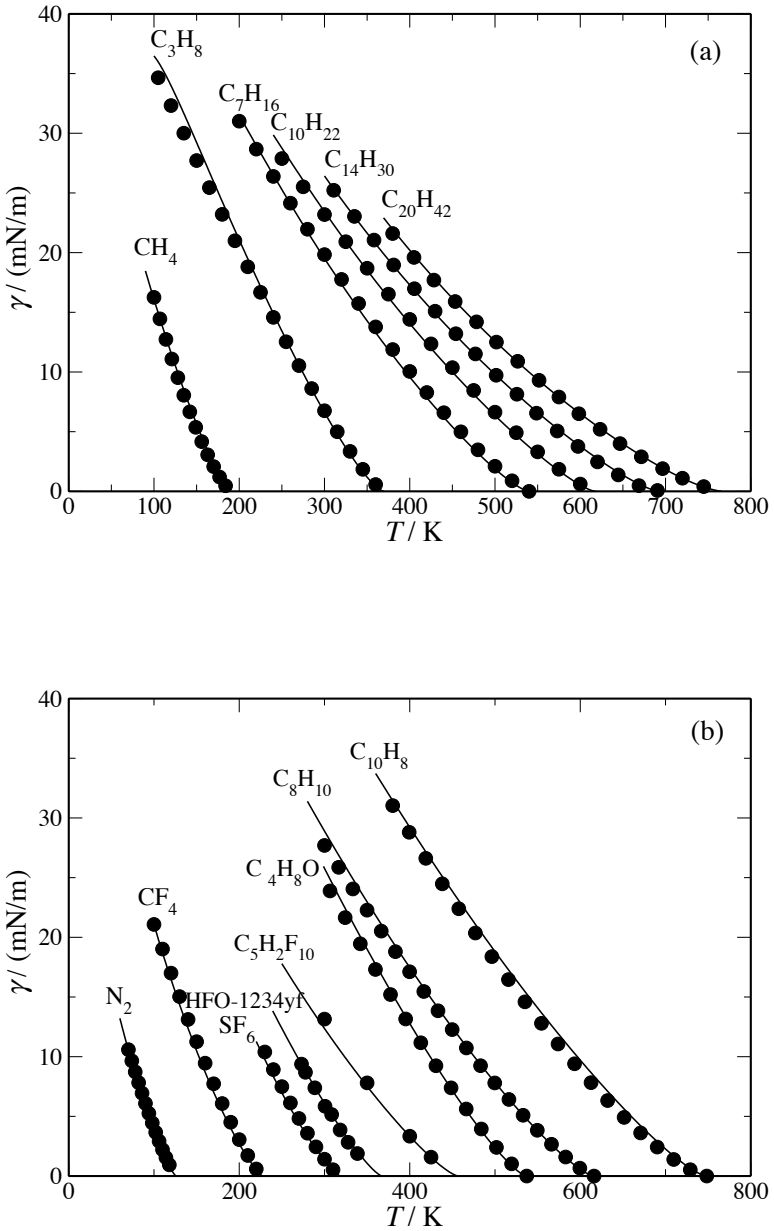
(a)
C3H8
C7H16
C10H22
C14H30
C20H42
CH4
γ / (mN/m)
T / K
0
10
20
30
40
0
100
200
300
400
500
600
700
800
(b)
C10H8
C8H10
C4H8O
CF4
C5H2F10
HFO-1234yf
N2
SF6
γ / (mN/m)
T / K
0
10
20
30
40
0
200
400
600
800

FIG. 5

TABLE I: Force field parameters for some Coarse Grained Mie $\lambda - 6$ fluids.

Fluid	m_s	ε/k_B (K)	σ (A)	λ	α	$10^{-20} \times c$ ($\mathrm{Jm^5mol^{-2}}$)
Methane (CH_4)	1	170.75	3.752	16.39	0.729	1.921
Propane (C_2H_6)	1	426.08	4.929	34.29	0.518	10.387
Sulfur Hexafluoride (SF_6)	1	389.10	4.898	43.97	0.490	8.015
Tetrafluoromethane (CF_4)	1	269.37	4.381	38.34	0.510	3.415
Nitrogen (N_2)	1	122.85	3.753	20.02	0.656	1.140
Hexane (C_6H_{14})	2	376.35	4.508	19.26	0.669	36.182
Heptane (C_7H_{16})	2	436.13	4.766	23.81	0.606	46.227
Naphthalene ($C_{10}H_8$)	2	557.75	4.623	19.50	0.665	60.132
p-Xylene (C_8H_{10})	2	475.76	4.524	21.17	0.639	42.889
HFO-1234yf ($C_4H_2F_4$)	2	265.53	4.074	18.22	0.688	16.215
Butanal (C_4H_8O)	2	382.23	3.998	17.69	0.699	21.864
Decane ($C_{10}H_{22}$)	3	415.19	4.585	20.92	0.643	90.785
HFC ($C_5H_2F_{10}$)	3	279.42	4.068	17.36	0.706	39.963
Tetradecane ($C_{14}H_{30}$)	4	438.11	4.619	22.22	0.625	167.920
Eicosane ($C_{20}H_{42}$)	6	453.10	4.487	24.70	0.597	310.718

TABLE II: Average Absolute Deviation for the interfacial tension (%AADγ)[a] reported in this work and some corresponding state correlations to the experimental data.

Fluid	%ADDγ[b]	%ADDγ[c]	%ADDγ[d]	%ADDγ[e]	%ADDγ[f]	%ADDγ[g]
Methane (CH_4)	0.94	4.73	2.64	6.97	2.34	2.21
Propane (C_2H_6)	1.23	6.16	2.71	7.19	2.89	4.78
Sulfur Hexafluoride (SF_6)	8.74	12.34	12.32	16.87	4.38	3.32
Tetrafluoromethane (CF_4)	22.64	21.62	21.84	20.88	18.24	1.93
Nitrogen (N_2)	4.36	5.27	3.07	19.61	2.79	0.79
Hexane (C_6H_{14})	1.25	6.38	2.08	5.77	2.63	0.82
Heptane (C_7H_{16})	1.99	6.86	2.37	6.21	2.32	1.95
Naphthalene ($C_{10}H_8$)	12.12	19.62	12.04	12.53	12.94	3.55
p-Xylene (C_8H_{10})	5.33	9.85	5.62	4.10	6.68	3.03
HFO-1234yf ($C_4H_2F_4$)	4.25	6.87	4.89	7.14	5.13	2.98
Butanal (C_4H_8O)	2.47	3.87	2.87	3.87	4.48	4.31
Decane ($C_{10}H_{22}$)	7.52	11.32	9.26	10.25	7.91	1.22
HFC ($C_5H_2F_{10}$)	6.84	10.24	7.14	9.87	7.54	3.23
Tetradecane ($C_{14}H_{30}$)	11.53	16.57	14.21	18.63	9.49	0.97
Eicosane ($C_{20}H_{42}$)	20.89	35.69	18.91	38.64	14.92	0.72
	7.47	11.83	8.13	12.57	6.98	2.39

[a] %AAD$\gamma = \frac{1}{N_P}\sum_i^{N_P}\left|\frac{\gamma_i^{exp}-\gamma_i^{calc}}{\gamma_i^{exp}}\right| \times 100$, where exp. denotes experimental data taken from DECHEMA[136], cal. represents calculated values, and Np corresponds to data points which are taken from the triple point to the critical point

[b] Brock and Bird[129]

[c] Curl and Pitzer[130]

[d] Zuo and Stenby[131]

[e] Sastri and Rao[132]

[f] Miqueu *et al.*[135]

[g] This work